LA-4931-MS
Informal Report
UC-28 & UC-48
ISSUED: August 1972

los alamos
scientific laboratory
of the University of California
LOS ALAMOS, NEW MEXICO 87544

Physical and Radiobiological Aspects of π^- Mesons in Radiotherapy

by

Mudundi R. Raju

los alamos
scientific laboratory
of the University of California
LOS ALAMOS, NEW MEXICO 87544

LA-4931-MS
Informal Report
UC-28 & UC-48
ISSUED: August 1972

Physical and Radiobiological Aspects of π^- Mesons in Radiotherapy

by

Mudundi R. Raju

PHYSICAL AND RADIOBIOLOGICAL ASPECTS OF π^- MESONS IN RADIOTHERAPY

by

M. R. Raju

ABSTRACT

The object of radiation therapy is to sterilize all cancer cells in a tumor-suspected volume yet make it possible for the normal vital structures within that volume to survive and repopulate it. In addition, radiation damage to exposed normal tissues must be kept to a minimum. This paper discusses the application of π^- mesons to these problems. The results of physical and radiobiological measurements of π^- mesons with reference to therapy, current plans for using π^- mesons in therapy, and problems associated with evaluating their potential are discussed.

I. INTRODUCTION

Radiation therapy and surgery are the two main forms of cancer treatment. In radiation therapy, tissue integrity is preserved as much as possible whereas in surgery all areas of tumor and tumor-suspected volumes will be taken out. Nearly 50% of all cancer patients receive radiotherapy at some stage of treatment. During radiation therapy, one would like to give as much dose as possible to the tumor volume while keeping the dose to the normal tissues outside the treatment volume as low as possible. Ideally, radiotherapists would like to give tumoricidal dose to the tumor-suspected volume, i.e., the dose necessary to kill all the tumor cells that are capable of cell multiplication. In practice however, the dose that can be delivered to the tumor volume is restricted by the injury done to the normal tissue, both within and outside the treatment volume. Normal tissue injury depends on the volume irradiated; the smaller the volume, the greater the dose the normal tissue can likely withstand. It must be noted that the normal tissue injury and volume are also related to the time taken to give the total dose.

With the advent of megavoltage sources over the past twenty years, it is now possible, for example, to cure permanently nearly 60% of the patients with locally inoperable cancer of the prostate.[1] Similar improvements have also been made in treatment of many other types of cancers. With the availability of megavoltage sources of radiation, the normal tissue injury outside the treatment volume is no longer a serious problem. However, radiations that could limit the high-dose region as closely as possible to the tumor volume are still of potential interest in radiation therapy. Although further improvements in dose localization by means other than megavoltage sources may not dramatically improve the cure rates, they could certainly be expected to reduce the complications that arise after radiotherapy.

It must be pointed out that the treatment volume, i.e., the tumor-suspected volume, comprises a considerable part of normal tissues. These normal tissues have to survive so that the patient can live in comfort, free from disease after the treatment. The use of radiation therapy in cancer management lies in the possibility of being able to let these normal tissues within the treatment volume survive and yet sterilize all the cancer cells. If the patient could survive without those normal tissues within the tumor-suspected volume, we would not need radiation; surgery could do the job.

Significant progress has been made in radiation therapy over the past two decades. This progress is mainly due to better understanding of the biology of cancer, better dosimetry, and use of high energy radiations in therapy. In spite of these developments, cure failure is still common. Suit[2] has estimated that, of 175,000 cancer deaths per year occurring in the United States despite treatment with radiotherapy, nearly 58,000 can be attributed to local or regional failure. Cure failure is generally due to the inability to give tumoricidal doses (doses necessary to sterilize all cancer cells) without undue effects on normal tissues within the treatment volume.

The critical margin between the tumor control and production of complications is illustrated in Fig. 1.[3] You can see from the figure that the complications restrict the dose to be given to tumor volume for increased tumor control. If we could displace the tumor control curve to lower doses and/or decrease the damage to normal tissue within and outside the treatment volume, thereby placing the complications curve to higher doses, one could expect further improvements in radiation therapy.

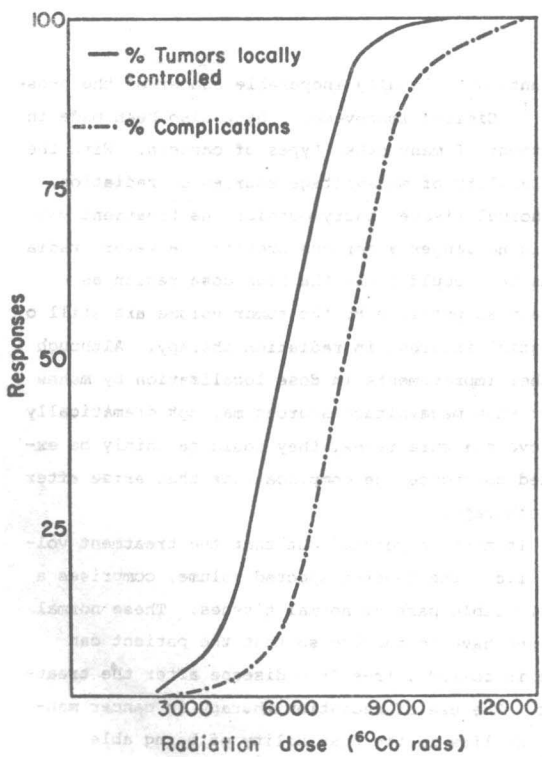

Fig. 1. General relationship between probability of local tumor control and production of complications as a function of ^{60}Co dose in rads.[3]

II. OXYGEN EFFECT

The object of radiation therapy is to sterilize all cancer cells in the treatment volume yet make it possible for the normal vital structures within the treatment volume to survive and eventually repopulate this volume. In spite of the availability of high-energy radiations and better dose localization characteristics, the question arises - what is preventing us from obtaining this balance? Gray[4] postulated that hypoxia may be an important cause of conventional radiotherapy cure failure. Many tumors have inadequate blood supply, hence they may contain a small proportion of hypoxic cells (cells lacking a sufficient supply of oxygen). For conventional radiation, the dose required to sterilize hypoxic cells is about three times that for oxygenated cells. The presence of hypoxic cells in the tumor therefore requires an increase in the tumoricidal dose. This is illustrated in Fig. 2.[5] The dose necessary to cure a tumor with 90% probability is given for oxygenated cells, 1% anoxic cells, and 100% anoxic cells. As you can see in Fig. 2, if all the cells are fully oxygenated, a 75 mm diam tumor could be cured with a dose of about 4,500 rads, but if a tumor of even 5 mm in diam contains 1% of anoxic cells it cannot be cured. Hence, when low LET* radiations are used, any further developments in dose distributions, however neatly tailored to the treatment volume, cannot avoid damage to normal tissues that are within the tumor volume because of the presence of even a small percentage of hypoxic cells.

It is known however, that in certain types of animal tumors, therefore probably in human tumors as well, an increasing proportion of hypoxic cells of the tumor becomes oxygenated during fractionated radiotherapy.[6] Thus, the hypoxic cells that are oxygenated during the treatment are not so resistant to subsequent fractions of radiotherapy. It may therefore be possible to overcome the oxygen

*The term LET is used very often in radiobiology and radiotherapy literature. It stands for linear energy transfer and is normally expressed in keV/μ of tissues. For water, 1 keV/μ = 10 MeV $g^{-1}cm^2$.

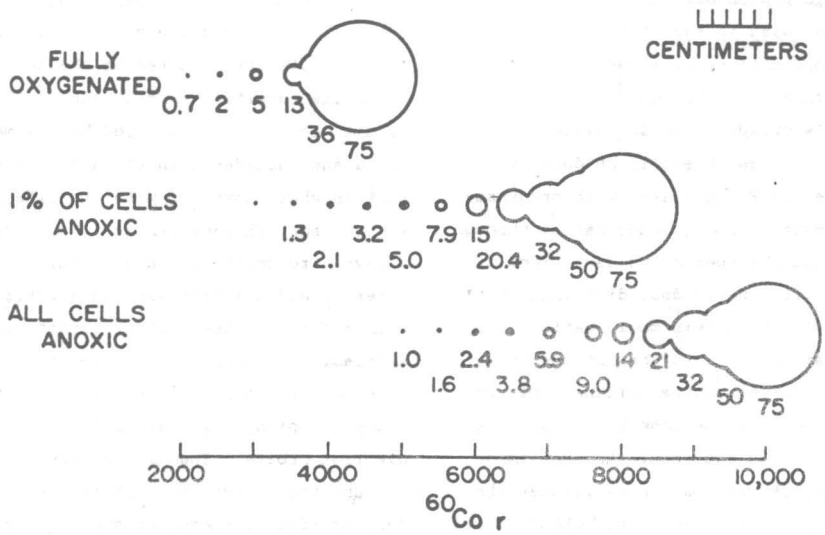

Fig. 2. Calculated doses required to reduce the number of cells surviving in each tumor volume to 0.1, to give a 90% chance of "cure."[5]

effect by fractionation with conventional low LET radiations alone for some less advanced stages of cancer. However, reoxygenation may not take place for advanced tumors. The radiation resistance of hypoxic cells when, compared to oxygenated cells, is reduced with increasing ionization density (dE/dx or LET). Thus, high LET radiations may be more effective in overcoming the hypoxic cell problem where the current methods are not successful. However, it must be pointed out that hypoxic cells, as a limiting factor in radiation therapy, are so far proven radiobiologically but not clinically.[7]

The physical and radiobiological properties of π^- mesons could be used to overcome some of the problems experienced in conventional radiation therapy.

III. PHYSICAL ASPECTS OF π^- MESONS

The depth dose distributions of different radiations could be broadly classified in two categories; one in which the dose decreases as a function of depth in the medium, the other in which the dose increases with the depth, giving rise to a sharp increase near the end of the range due to the Bragg peak effect. High-energy x rays, gamma rays, and fast neutrons belong to the first category whereas heavy charged particles, i.e., protons, heavy ions, and π^- mesons belong to the second category.

A π^- meson has approximately 15% of the mass of a proton. It shares the properties of heavy charged particles. The depth-dose distribution of π^- mesons is similar to that of heavy charged particles. Figure 3 shows the depth-dose distribution

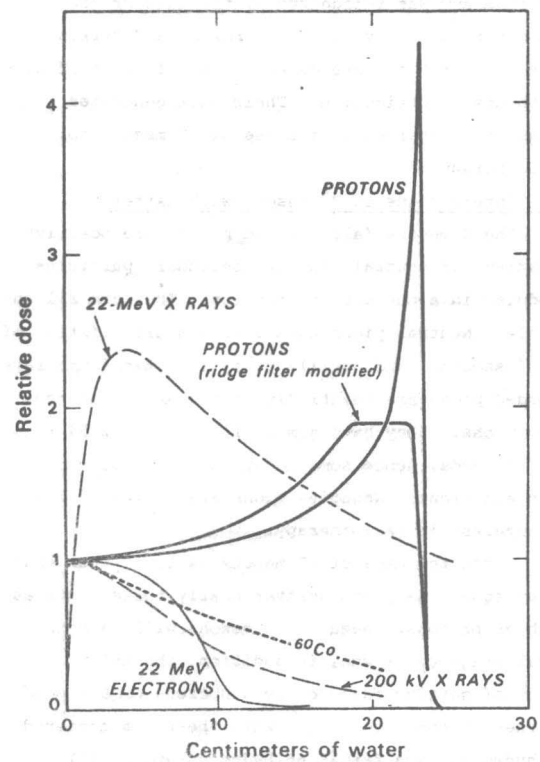

Fig. 3. Depth-dose distributions of protons, electrons, x rays, and γ rays.

of the monoenergetic proton beam compared with conventional radiations used in radiation therapy. For radiotherapeutic applications it is necessary to modify this depth-dose distribution so that this narrow Bragg peak is broadened to irradiate a large volume uniformly. This could easily be done by overlapping a series of Bragg peaks, with progressively smaller intensities and shorter ranges through the use of a variable absorber known as a ridge filter.[8,9] Such a modified depth-dose distribution is also shown in Fig. 3. With this modification, the ratio of the dose at the peak to that at the entrance is reduced with increasing thickness of the treatment volume; however, the dose at the peak is always higher than at the entrance. Another important aspect of heavy charged particles is that the dose beyond the range is very small and the fall-off very sharp. Thus, from physical considerations, heavy charged particles surpass conventional radiations and fast neutrons in delivering large doses to deep-seated tumors with minimum dose to the surrounding normal tissue.

The potential application of negative pions in radiotherapy was recognized by the late Dr. Fermi and others as early as 1950. Fowler and Perkins[10] were the first to make detailed calculations of pion depth-dose distribution. Their work generated heightened interest in the use of π^- mesons for radiotherapy.

A. Interactions of π^- Mesons with Matter

The π mesons (also called pions) are positive, negative, or neutral, and are secondary particles produced in a nuclear interaction. They are all unstable. Neutral pions have a very short lifetime of 10^{-16} seconds, and usually decay into two gamma rays. Charged pions are relatively more stable than neutral pions. They have a mean lifetime of 2.54×10^{-8} seconds, hence some decay in flight to muons then electrons. Negative pions are the particles of interest in radiotherapy.

Since the mass of π^- mesons is lower than that of protons, the pions scatter nearly three times as much as protons. Negative π mesons will have the usual Bragg curve and, in addition, the unique property of getting captured by a nucleus of the medium when it comes to rest. When the π^- is captured by hydrogen, the resulting hydrogen atoms will have π^- in the electronic orbit in place of the electron. The hydrogen atom diffuses through the medium. When this atom gets close to a heavier nucleus, the pion is often transferred to the heavier atom because the resulting binding energy is lower. As a result, the pion is captured by the main tissue elements and cascades down the atomic levels in a time that is short compared with its lifetime. During the cascade, characteristic x rays, called π mesic x rays, are emitted. These x rays are of special interest and are discussed in a later section. The π^-, when in the lower atomic orbit, spends a considerable fraction of the time inside the nucleus (its mass being 273 times that of an electron) because the pion orbits are only 1 x 273 as large as electron orbits. The pion is absorbed by the nucleus, and the π^- rest mass of 140 MeV appears in the form of kinetic energy of nuclear fragments, except for about 40 MeV, which is used in overcoming the

Fig. 4. Examples of capture of negative pions and the resulting nuclear disintegrations in the light elements carbon, nitrogen, and oxygen as observed in nuclear emulsions. The pion traces are labeled π^-; the stars produced following their capture have various numbers of prongs.

the binding energy of the nucleus. Nearly 70 MeV appear in the form of kinetic energy of neutrons, and the rest (about 30 MeV) in the form of kinetic energy of the charged particles, such as protons, alpha particles, and heavier particles that are absorbed locally.[10] Thus, for π^-, the capture process enhances the dose near the Bragg peak region due to these short-range and heavily-ionizing fragments. In addition, these highly ionizing fragments are expected to overcome the hypoxic cell problem considerably. It is this unique characteristic of the π^- that makes it promising in radiotherapy. Examples of π^- capture as observed in a nuclear emulsion are shown in Fig. 4. The disruption of the nucleus is often referred to as "star formations."

In bone-free parts of the body, about 73% of π^- mesons are captured in oxygen, 20% in cargon, 3% in nitrogen, and 4% in heavier atoms.[11] Fowler and Mayes found that interactions with oxygen produced various tracks due to particles of different charges. Some of the dominant reactions in oxygen are:

$$\pi^- + {}^{16}O \rightarrow {}^{12}C + p + 3n,$$
$$\rightarrow 3\alpha + p + 3n,$$
$$\rightarrow {}^{14}N + 2n,$$
$$\rightarrow {}^{10}B + \alpha + 2n.$$

The type of the particle, its energy, and frequency per capture in water, as measured by Fowler and Mayes are shown in Table I.

TABLE I.

ENERGY PARTITION FOR π^- CAPTURE IN WATER

Particle Type	Average Energy per Pion Star (MeV)	Average Number of Particles per Pion Stars
Protons	15.2	0.95
Deuterons	- -	- -
α Particles	7.8	0.99
Heavy recoils $Z \geq 3$	4.4	0.78
Neutrons	69.0	2.7

The capture reactions in carbon, nitrogen, and oxygen are quite similar in their yield of protons and alpha particles and their mean energies. The energy spectrum of each type of particle covers a wide range.

The phenomenon of pion capture, on the average, yields one singly-charged particle (protons, deuterons, or tritons), one alpha particle, one heavy particle ($Z \geq 3$), and three neutrons. The dose contributed locally by the neutrons is small compared with the other components in the star. Although protons contribute considerable dose, alpha particles produce considerable biological effect. Heavy recoils also produce significant biological effect, since their ranges extend up to 20 microns in tissue, with an average of about 8 microns.

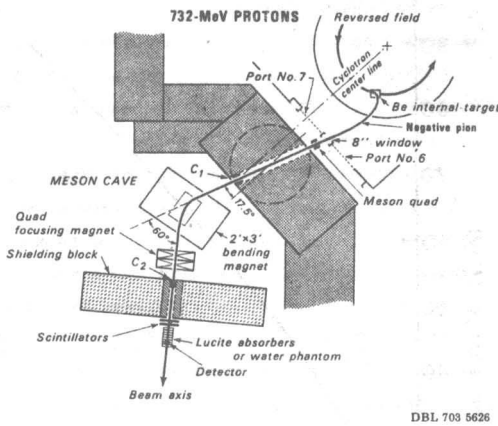

Fig. 5. Experimental set-up for producing a pion beam.

About 2% of stopping pions produce high-energy gamma rays, peaking in the energy region of about 100 MeV.[12] These gamma rays are of special interest and are discussed more fully later.

B. Production of Pions with Protons

A brief description of pion production at the 184-in. cyclotron at Berkeley will provide more information about a pion beam and its composition. The setup is shown in Fig. 5. The accelerated protons from this accelerator strike a beryllium target and produce π^-, π^+, and π^0. The π^- mesons are deflected out of the cyclotron through a vacuum window by the cyclotron fringe field, which works as the first bending magnet. The beam is then focused by a quadrupole focusing magnet (meson quad) and passes along a channel through the main cyclotron shielding (dotted area). The energy of the beam is selected by adjusting the current in the bending magnet, and the beam is focused again by another quadrupole focusing magnet.

C. Pion Beam Contamination

Neutral pions produced in the target decay into two gamma rays because of their short lifetime of

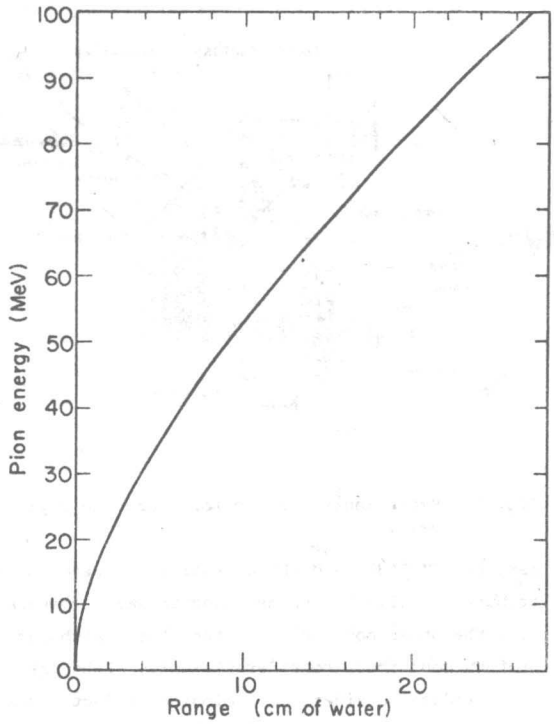

Fig. 6. Range vs. energy for pions in water.

10^{-16} sec. The gamma rays are converted into electron-positron pairs in the target. The electrons from this conversion constitute the electron background in the π^- beam. Charged pions have a mean life of 2.54×10^{-8} sec, hence some of them decay in flight; contributing the muon background. The muons and electrons that have the same momentum as the pions selected by the bending magnet remain in the beam. The range of muons is about 30% greater than pions of the same momentum, and the electrons have a much higher range. For a beam of momentum 140 MeV/c, the range of π^- is ~12 cm of water, π^- ~16 cm, and e^- >> 30 cm. The muon and electron contamination in a pion beam could be reduced by using radiofrequency or electrostatic separators. These separators select particles according to velocity.

D. Range Energy

The range of π^- in water, as a function of energy, is shown in Fig. 6. In radiation therapy, pions with energies from ~40 to 70 MeV are of interest. The momentum of a particle is often used in high energy physics in addition to energy. The energy selection of particle beams is done by magnetic

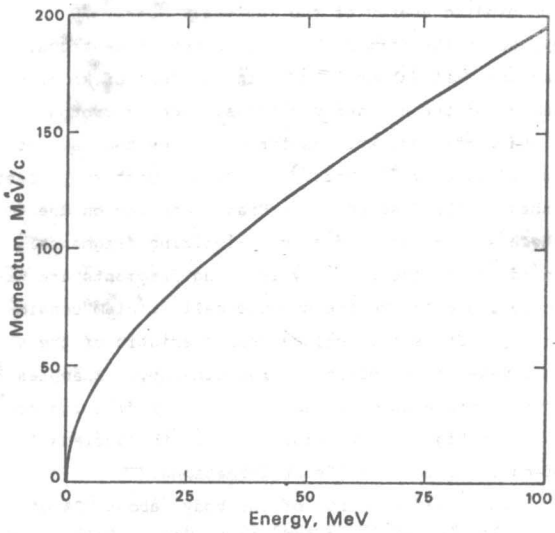

Fig. 7. Energy vs. momentum for pions.

fields, and the deflection of a particle in a given magnetic field is proportional to its momentum. The plot of energy versus momentum for pions is shown in Fig. 7.

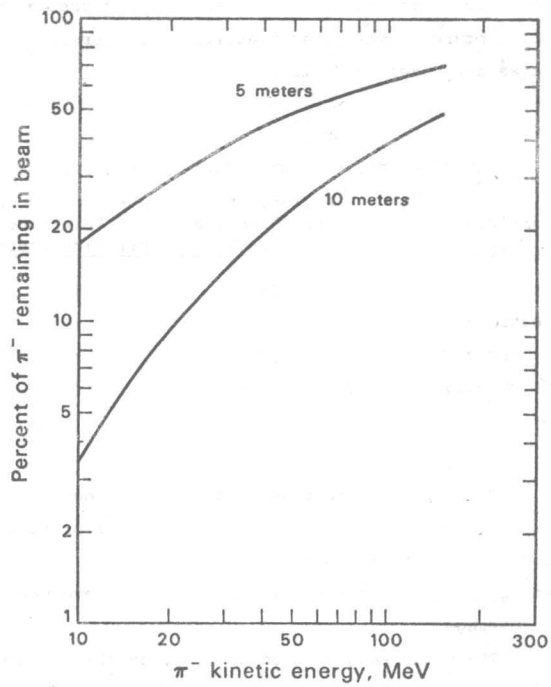

Fig. 8. Percentage of original π^- flux remaining after a 10-m and 5-m drift.

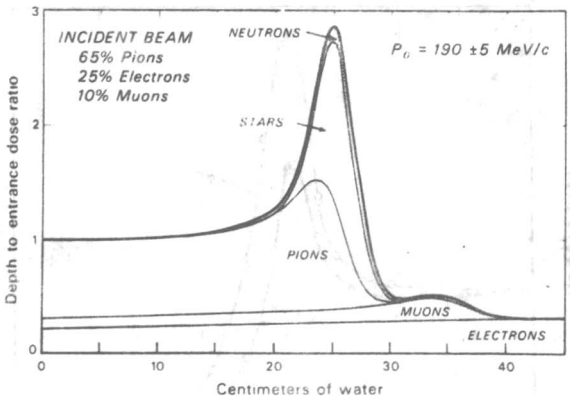

Fig. 9. A normalized central-axis depth-dose curve in water for an incident beam of π^- of momentum 190± 5 MeV/c with contamination (65% π^-, 25% e^-, 10% μ^-).

E. Pion Decay

A distance of about 5 to 10 meters between the target and the experimental area is generally required to allow the necessary shielding against the intense flux of neutrons and gamma rays produced in the target and to accomodate the magnetic system needed to deliver pions of the desired energy to the experimental area. Low-energy pions decay much faster than high-energy pions. Figure 8 shows the percentage of original π^- remaining in the beam after it has traveled about 5 and 10 m. Figure 8 shows that nearly 75 and 50% of pions, in the energy range of interest to radiotherapy, decay in flight in drifting to a distance of 10 and 5 m, respectively. The resulting

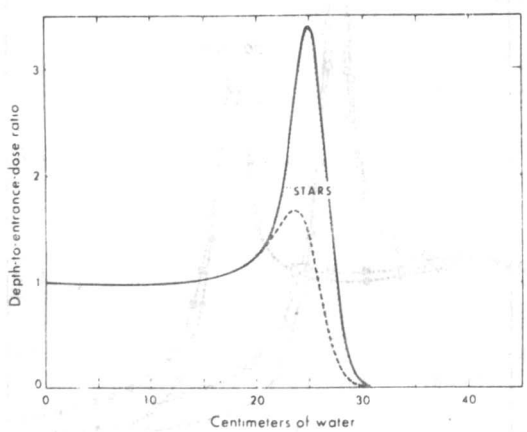

Fig. 10. A normalized central-axis depth-dose curve in water for an incident beam of π^- of momentum 190± 5 MeV/c (pure beam).

muons have a broad energy spectrum. Muons having the same momentum as pions selected by the magnetic system remain in the beam as contamination. Because of this decay it is not practical to use energies much lower than about 40 MeV. Even for a short beam path of about 5 m, nearly 50% of the mesons decay. Hence, if we want to consider using π^- mesons in therapy, it is very important to have as intense a primary beam as possible. In addition, it is necessary to collect pions from the target over as large a solid angle as possible.

F. Depth-Dose and LET Distribution of π^- Mesons

The pion depth-dose distributions as calculated by Curtis[13] for a 95 MeV beam with a contamination of 10% π^- and 25% e^-, and for a beam with no contamination, are shown in Figs. 9 and 10, respectively. Electron and muon contaminations in the beam reduce the peak-to-plateau ratio and contribute dose beyond the treatment volume. The LET distribution of π^- at the peak of depth-dose distribution in water is shown in Fig. 11. The figure also shows contributions from the various components of the beam. The area under the curve is proportional to the dose. The figure shows that even at the peak of depth-dose distribution, a substantial part of the total dose is due to

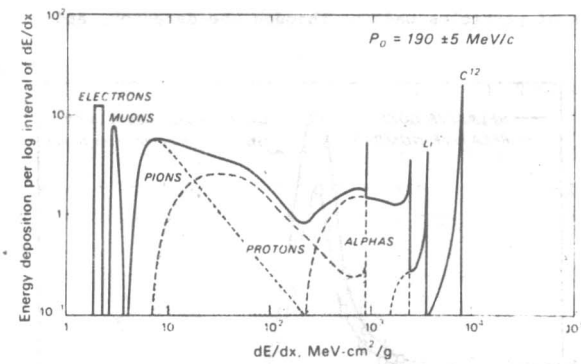

Fig. 11. The dE/dx distribution of a contaminated π^- beam at the peak of depth-dose distribution (25.5 cm of water). Calculated for an incident gaussianly distributed momentum distribution 190± 5 MeV/c. The contribution of each component is shown. The beam was assumed to be composed initially of 65% π^-, 25% electrons, and 10% muons. (The energy lost by a particle in traveling through a unit distance is called linear energy loss and is usually denoted by dE/dx expressed in MeV.$g^{-1}cm^2$. Sometimes it is expressed in keV/μ. In water 10 MeV.$g^{-1}cm^2$ = 1 keV/μ.)

pions that are still slowing down. Most of the protons from star formation are of low LET. The alpha particles and heavy recoils are of high LET, the latter extending up to 900 keV/μ. For a pure pion beam the percent dose contribution at the peak of the depth-dose distribution, due to pions passing the peak, is 35%; that due to protons from stars is 33%; that due to heavily ionizing components, such as alpha particles and heavy recoils, is 25%; and that due to neutrons is about 7%. Thus, at the peak region, the component due to LET values greater than 30 keV/μ is about 30%, varying significantly over the peak region. This high LET component decreases with increasing width of the Bragg peak.

Physical measurements have been carried out at the 184-in. synchrocyclotron at Berkeley[14] and at the CERN synchrocyclotron at Geneva.[15] Some measurements were also made at the Brookhaven cosmotron.[16] Lithium drifted silicon detectors were used to obtain integral range curves and depth-dose distributions for π^- mesons.[14] The detector was housed in an electrically shielded Lucite box, and was remotely positioned in a water phantom. By using a time of flight system in conjunction with the silicon detector system, the information for a pure pion beam was also obtained. By plotting the total number of particles passing through the detector, and

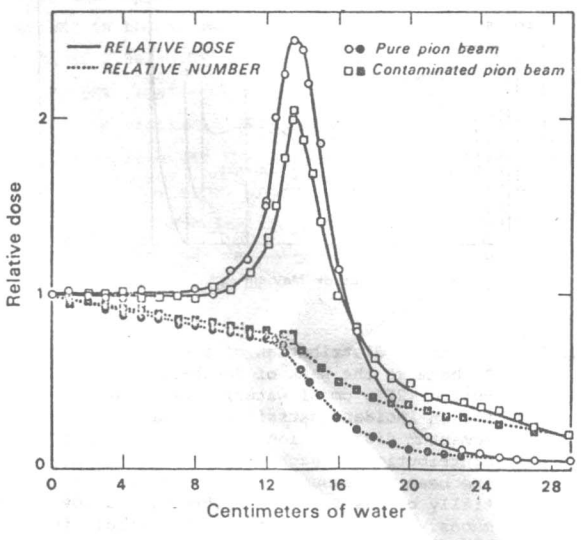

Fig. 12. Number-distance (integral range) curves and depth-dose distribution of 65 MeV π^- beam in water.

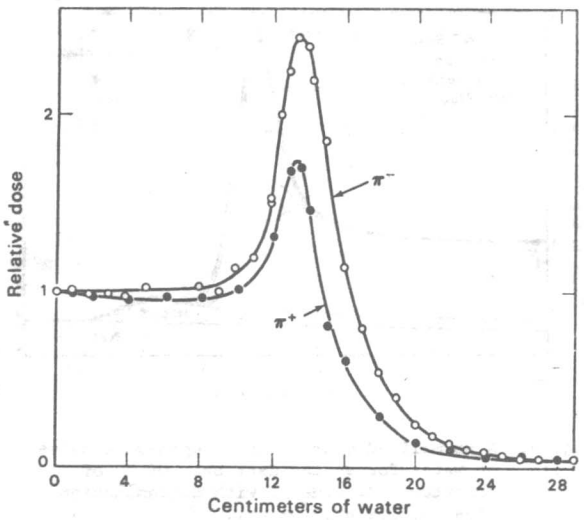

Fig. 13. Depth-dose distribution of 65 MeV π^- and π^+ pure beams in water.

the total energy deposited by them as a function of depth in water, we obtain the integral range and depth dose curves respectively. Figure 12 shows such curves, both for contaminated and pure 65 MeV π^- beams.

To evaluate the dose distribution due to π^- stars, the depth dose distributions in water of pure 65 MeV π^- and π^+ meson beams were measured. The results are shown in Fig. 13. The increase in dose

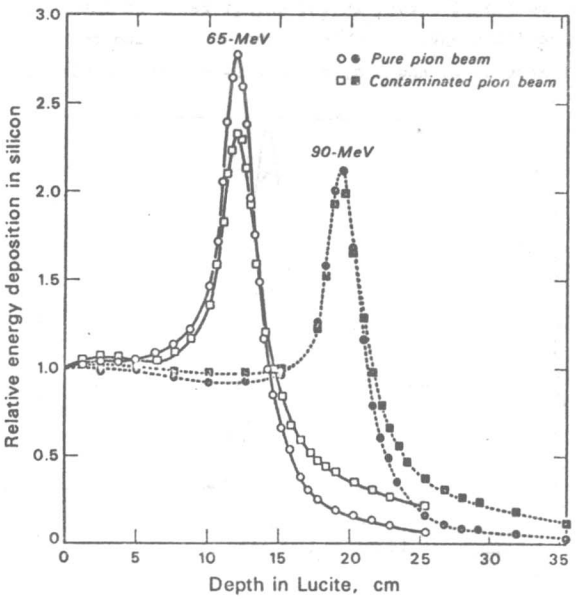

Fig. 14. Depth-dose distribution of 65 MeV and 90 MeV π^- beams in Lucite.

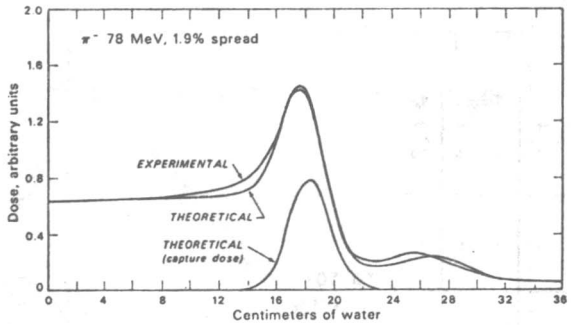

Fig. 15. Depth-dose distribution of 167.5 MeV/c π^- spread.[17]

for the π^- beam at the peak region is due to star events. This difference could be slightly greater if it were not for a small contribution by muons and positrons resulting from π^+ decay. Nearly 50% of the dose at the peak of the depth-dose distribution is due to nuclear events.

The dose distribution for 65 and 90 MeV pion beams is shown in Fig. 14. The high-energy beam has a lower value of peak-to-plateau ratio mainly due to loss of particles by nuclear attenuation and multiple scattering before reaching the end of the range.

The depth-dose distribution of π^- mesons measured at CERN, Switzerland are in good agreement with our experimental values obtained at Berkeley. Figure 15 shows the results of the CERN experimental results compared with theoretical calculations.[17] The agreement between theoretical calculations and the experimental results are very good.

As discussed before, π mesic x rays and γ rays are also emitted from the region where the π^- stop and produce stars. The dose contribution from x rays and γ rays is small. However, significant numbers of π mesic x rays and γ rays can be detected outside the exposed patient. This radiation may provide a good method of externally observing the stopping pion region to aid in planning treatment and monitoring during exposure. Experimental results indicate this can indeed be done in principle.[18,19]

High-energy γ rays coming out of a phantom were detected by spark chambers and are shown in Fig. 16. The peak of the γ rays corresponds to the peak of depth-dose distribution. By adding 6-mm-thick Lucite sheets in front of the phantom, the peak is found to shift by the corresponding amount. The γ rays on the extreme side of the peak are produced by the nuclear interaction of pions in flight.

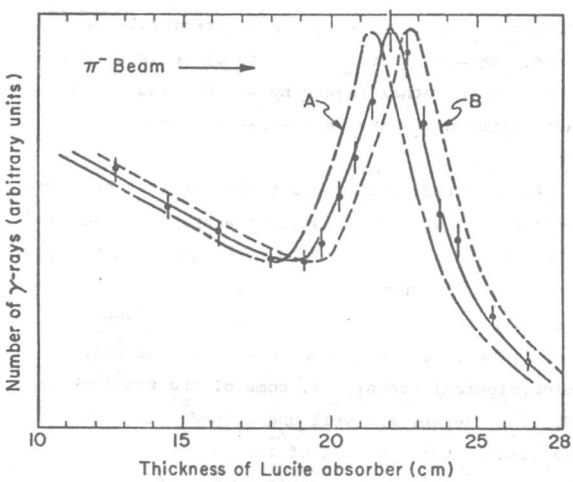

Fig. 16. Number of γ rays as a function of Lucite absorber thickness. Curve A is obtained by placing an additional 6 mm of Lucite in front of the phantom and Curve B by removing 6 mm of Lucite.

IV. RADIOBIOLOGICAL ASPECTS OF π^- MESONS

Before presenting the radiobiological data on π^- mesons, I will briefly discuss some of the radiobiological techniques and the current concepts of radiation biology with reference to radiation therapy.

T. T. Puck developed the technique of growing mammalian cells outside the body (in vitro) in an artificial environment. Using Puck's method, cells have been cultured for about a week or two, each individual surviving cell divides many times and a

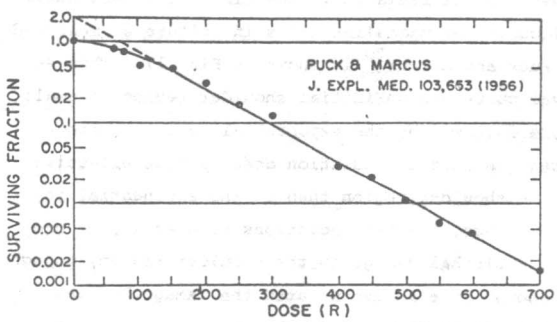

Fig. 17. Survival of reproductive capacity in the HeLa cells as a function of x ray dose.[20]

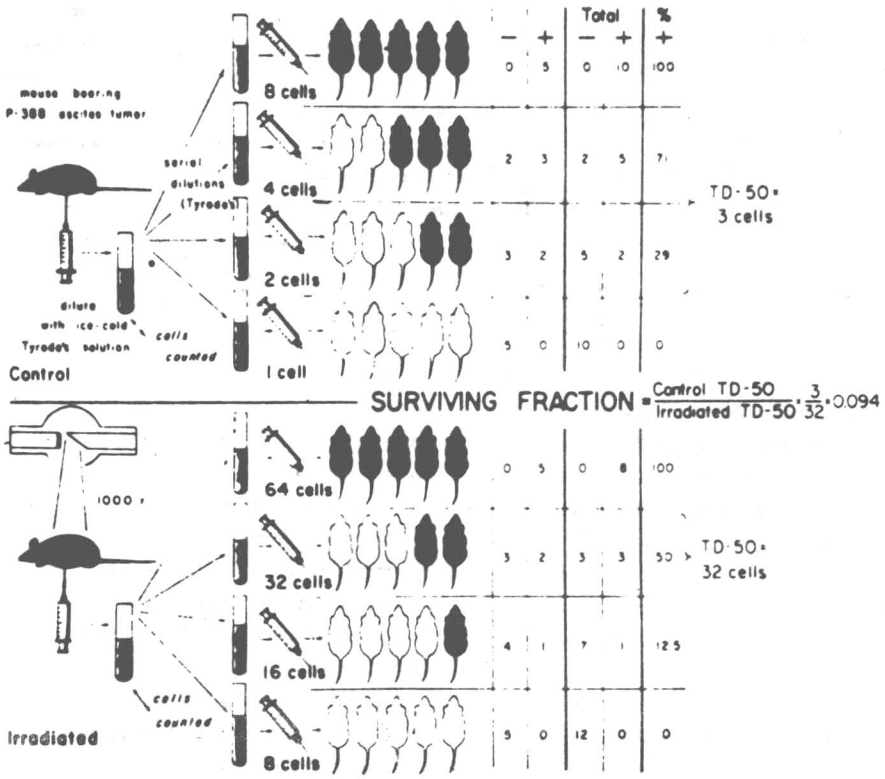

Fig. 18. Scheme for measuring cell survival in vivo as a function of dose.[41]

large number of cells (called a clone) appear in the place of every surviving cell. The clones can be seen with the naked eye. This technique makes it possible to measure the number of cells killed, either in the presence or absence of oxygen for a given dose of radiation. The first published survival curve for mammalian cells in culture as measured by Puck and Marcus[20] is shown in Fig. 17. This survival curve has an initial shoulder region of small slope followed by the exponential region at higher doses. A unit of radiation dose is less effective in the shoulder region than in the exponential region. Thus, low LET radiations such as x rays produce sublethal damage in the shoulder region; though if enough dose is accumulated the damage becomes lethal, as is the case in the exponential region. Elkind[21] has demonstrated for the first time that mammalian cells repair sublethal damage within a few hours, the cells that survive respond to subsequent radiation as if they had not been previously irradiated. Because of this capacity of cells to recover from sublethal injury by low LET radiations, fractionated doses are less effective than single doses.

Another radiobiological technique that has very significantly guided radiation therapy was developed by Hewitt and Wilson.[22] This technique permits us to measure cell survival inside the body of the mouse (in vivo). The principle of this technique is shown in Fig. 18. With the development of these radiobiological techniques, some of the problems in radiation therapy are well understood. In addition, some idea is being gained of the radiation doses necessary to sterilize a given number of cells. The cell survival curve as measured by Hewitt and Wilson is shown in Fig. 19. As you can see, one could go to much lower levels of survival using this technique when compared to the cell-culture techniques

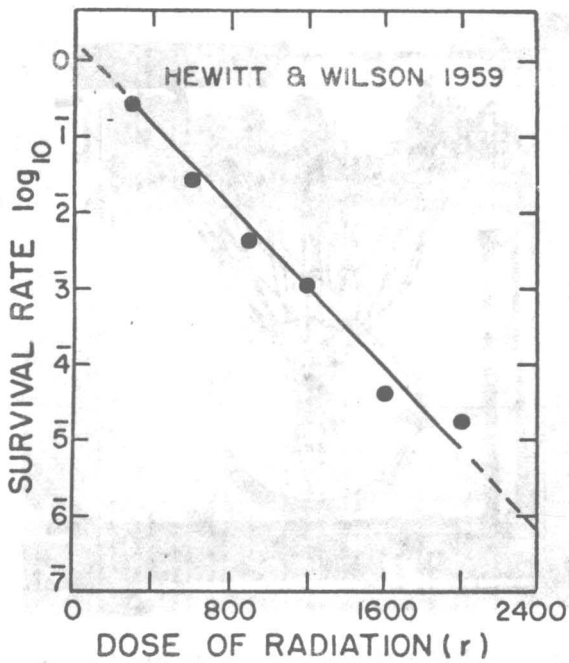

Fig. 19. Relationship between radiation dose and log survival rate among leukemia cells irradiated in vivo.[22]

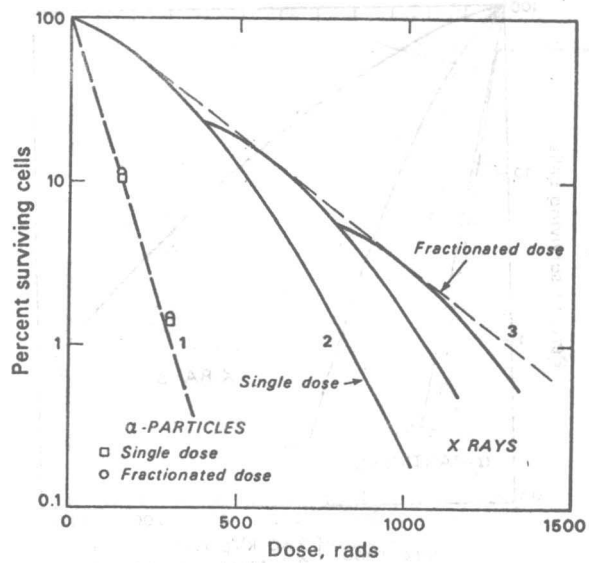

Fig. 20. Survival curves of human kidney cells (T_1) in culture.[24]

in vitro. Figure 20 shows the survival curves for x rays and 3.4 MeV alpha particles (LET on the order of 140 keV/μ) as measured by Barendsen.[23] In this figure, the survival curve for alpha particles has no shoulder. The lack of shoulder for alpha particles indicates that there is no sublethal damage. Thus, in the absence of cell growth, fractionated doses of low energy alpha particles are just as effective as single doses. Figure 20 also shows that the biological effect of low-energy alpha particles for a given dose of radiation is greater than that of x rays. The relative biological effectiveness (RBE) of a given radiation is defined as the ratio of x ray dose to that of the radiation in question required to produce the same biological effect. Thus, in this case the RBE of low-energy alpha particles is about 3. Because of changes in survival curves for high-LET radiations, the RBE for high-LET radiations varies depending on the survival level at which it is calculated.

Figure 21 shows the survival curves of x rays and alpha particles in the presence of air and nitrogen. The ratio of doses required to produce the same biological effect in the absence and presence of oxygen is commonly known as the oxygen enhancement ratio (OER). For x rays, this ratio is about 2.5 to 3, whereas for high-LET radiations, such as low-energy alpha particles, this ratio is very nearly 1.

Figure 22 shows changes in RBE and OER as a function of LET.[24] The figure shows that the RBE increases with LET, reaching a peak at about 100 keV/μ. Further increase in LET decreases the RBE because of saturation, i.e., the dose deposited is in excess of the dose necessary to kill the cells, and the excess energy is wasted. It must be pointed out that this relationship of RBE with LET depends on the type of cells used in the investigation. The OER decreases with increasing LET, reaching unity at about 150 keV/μ. Thus, when high-LET radiations are used for radiotherapeutic applications, there will be an increase in biological effect for a given dose of radiation when compared to x rays. In addition, the radiation protection of hypoxic cells will be less when compared to x rays. With this background in radiation biology let me briefly discuss some of the radiobiological measurements that have been made with π^- beams at Berkeley.

The current sources of negative π mesons do not have adequate intensity to do the necessary radiobiology and therapy with them. The Berkeley 184-in.

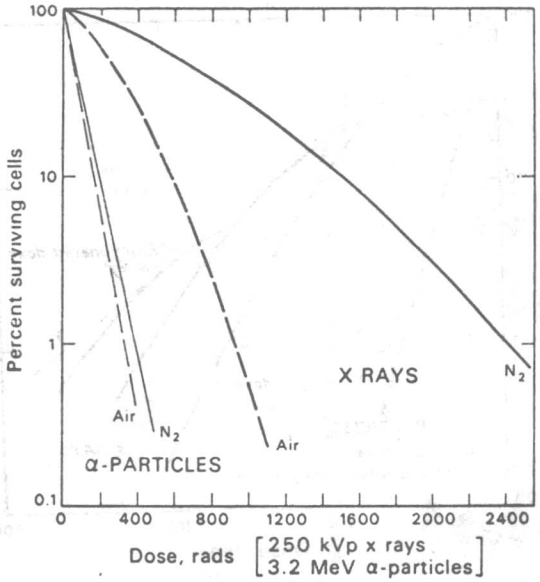

Fig. 21. Survival curves of x rays and ^{210}Po alpha particles with presence of air and nitrogen.[42]

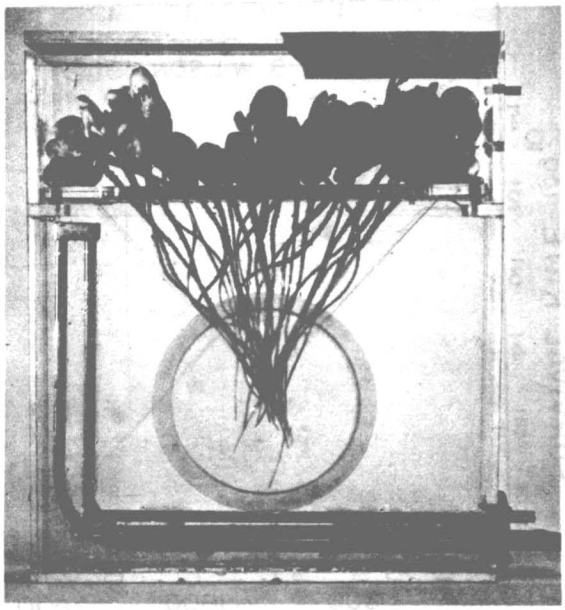

Fig. 23. Bean roots in a Lucite box used for π^- meson exposures.

synchrocyclotron is the most intense source of low-energy pions currently available. Even there the dose rates available are in the range of 5 to 60 rads/h at the peak, depending on the size of the beam. This intensity, however, is not adequate for the necessary pretherapeutic radiobiological work. Some measurements of RBE and OER have been made by using different biological systems that are sensitive enough for the intensity of the pion beam available. Most of these measurements have been made at only two points in the depth-dose distribution. The contaminated beam was used in all the radiobiological work since purification of the beam reduced the pion intensity considerably. The beam has a contamination of 25% electrons and 10% muons. At the beam entrance these contaminants deposit nearly 30% of the dose. At the peak the beam contamination deposits nearly 10 to 15% of the dose. Most of the radiobiological work has been published in the literature and some of the work is being published now. A summary of these results is given in Table II and III. As an example, I will briefly discuss the RBE

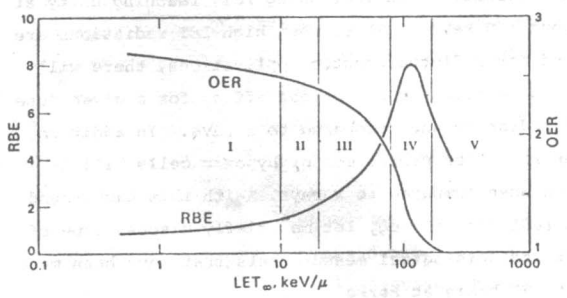

Fig. 22. The relations of RBE and OER with LET_∞ in different regions of LET, measured for damage to the reproductive capacity for cultured cells (T_1).[24]

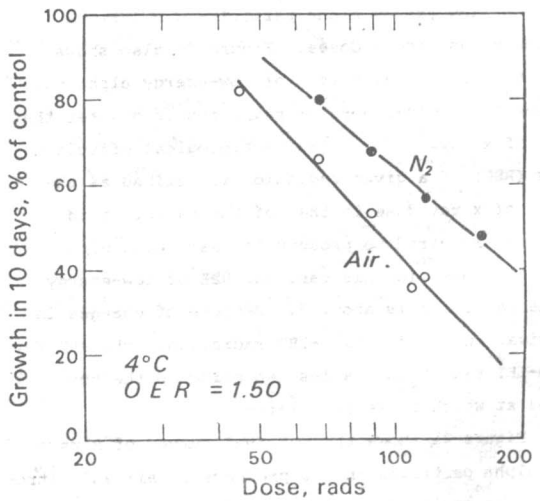

Fig. 24. The 10-day growth plotted as a function of dose at the peak of π^- beam.

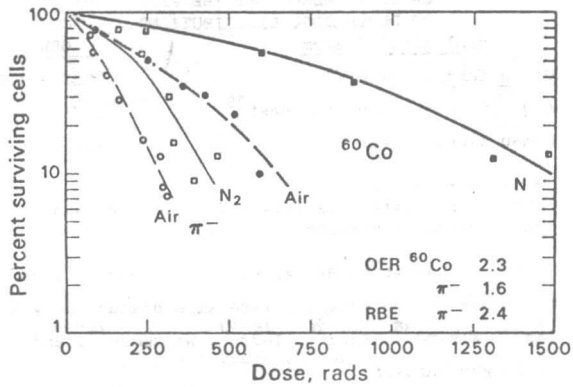

Fig. 25. Survival curves of human kidney cells in culture (T_1) for π^- mesons at the peak of the depth-dose distribution and for ^{60}Co γ rays.

and OER measurements at the pion peak using bean roots and human kidney cells in culture and the survival of ascites tumor cells measured in vivo using the technique by Hewitt and Wilson.[22]

The cells of the bean root tips respond to radiation in some respects (such as inhibition of cell division and production of chromosome damage) much as do human cells and a wide variety of organisms. The advantage of this material is economy, the ease with which it can be handled, and the avoidance of suffering which animals experience in radiation experiments. It is also possible to irradiate bean root tips under different conditions such as the presence or absence of oxygen. Figure 23 shows the bean roots in a Lucite box used for studying the difference in radiation damage from π^- mesons in the presence and absence of oxygen environment for π^- mesons. The difference in ten-day growth of exposed and unexposed bean root tips is an index of radiation damage. Figure 24 shows such a growth plot for bean roots exposed to π^- mesons in the presence of air and nitrogen at the peak position.[25] The OER was found to be 1.5.

Human kidney cell survival curves for π^- mesons at the peak in the presence of air or nitrogen are shown in Fig. 25. Also shown in the figure is the survival curve for ^{60}Co gamma rays at a dose rate such that the cell exposure was of the same duration

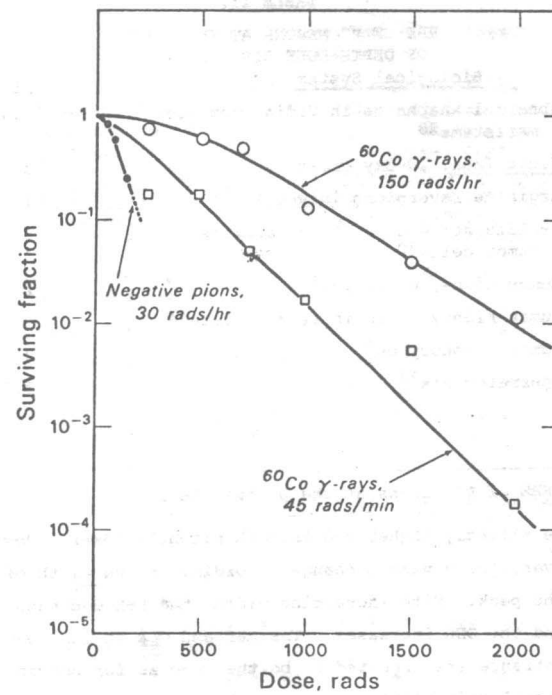

Fig. 26. Survival of 2-day-old lymphoma ascites tumors after low- and high-dose-rate irradiations with π^-, and ^{60}Co γ rays.

as for mesons. The dose rate of pions is about 25 rads/h, and the dose rate of ^{60}Co is about 1 rad/min. The RBE and OER for π^- mesons calculated at 10% level are 2.4 and 1.6 respectively.[26]

The proliferative capacity of ascites tumor cells irradiated in vivo in mice was measured by Feola.[27] The RBE of a 2-day-old ascites tumor cell was measured at the peak. The control experiments for ^{60}Co γ rays were also done at two dose rates, one at 150 rads/h and the other at 45 rads/min. The results are shown in Fig. 26. As you can see, the cell survival in this system depends considerably on dose rate. The RBE for pions, when compared to that of ^{60}Co γ rays at a dose rate of 150 rads/h was found to be about 5.

The biological results could be summarized by saying that, depending on the biological end point and the system used, the RBE value at the peak is in the region of two to five and the RBE at the plateau is nearly one.

The OER values at the peak of the depth-dose distribution are in the region of 1.5 to 1.8. For a pure pion beam, the RBE values at the peak will

TABLE II.

RBE OF π^- MESONS AT THE PEAK OF DEPTH-DOSE DISTRIBUTION[a]

Biological System	RBE
Abnormal anaphases in Vidia faba root meristems[28]	2.4
Vicia faba, 10-day growth[25]	3
Arginine reversions in yeast[29]	1.8
Proliferative capacity of ascites tumor cells[30]	5
Human kidney cells T-1[26]	2.4
Human kidney cells in frozen state[31]	~ 2
Human lymphocytes[32]	2
Spermatogonia[33]	3.7

[a] RBE of π^- mesons at the plateau is 1.

TABLE III.

OER OF π^- MESONS AT THE PEAK OF DEPTH-DOSE DISTRIBUTION[a]

Biological System	OER
Vicia faba (growth)[25]	1.35 - 1.5
Arginine reversions in yeast[29]	1.9
Human kidney cells T-1[26]	1.6

[a] OER at the plateau is expected to be the same as conventional radiation, i.e., 2.6.

be slightly higher and the OER slightly lower. However, these values change according to the width of the peak. With increasing width, the RBE decreases and the OER increases. The RBE and OER at the beam entrance are expected to be the same as for conventional radiations.

I have recently summarized in detail a chapter on physical and biological aspects of negative pions in radiotherapy which will be published in Current Topics in Radiation Research. The potential uses of π^- mesons in radiotherapy were also discussed by Kaplan[34], Elkind[35], Bond[36], Todd[37], Whitmore[38], and Feola and Maruyama.[39]

There is considerable interest now in the use of fast neutrons in radiation therapy. The dose localization characteristics of fast neutrons are inferior to most of the conventional sources of radiations used in radiotherapy. However, because of their higher LET, they are more effective than conventional radiations in killing hypoxic cells for a given dose to the oxygenated cells. Radiobiological measurements of fast neutrons indicate that the RBE for tumor tissues are higher than for normal tissues. Recent clinical results of fast neutrons at Hammersmith Hospital are encouraging and suggest

Fig. 27. Aerial view of LAMPF facility. (a. Laboratory - Office Building; b. Power Substation; c. Main equipment aisle; d. Operations Building; and e. Experimental area.

that high-LET radiations may have an important role in radiotherapy. The advantage of π^- mesons is that a high-LET dose, similar to the fast neutrons, is delivered only at the treatment volume and we could expect, on the basis of recent fast-neutron data, that the effect on tumor tissues is higher on normal tissues within the treatment volume.

The physical and radiobiological measurements of π^- mesons indicate that the intervening normal tissue receives low dose at an LET similar to that of conventional radiation. Also, the treatment volume receives higher dose at high LET which increases the biological effect there and, in addition, increases the damage to hypoxic cells. It is also noted that intervening normal tissues recover more than the cells in the treatment volume. Fractionation enhances the damage to the treatment volume when compared to the intervening normal tissues. Thus, π^- mesons offer the additional advantage of favorable biological factors due to differences in the quality of radiation.

Pion facilities with intensities adequate for therapy are being built at Los Alamos, New Mexico, Vancouver, B. C., and Zurich, Switzerland.[39,40] Figure 27 shows the Los Alamos Meson facility construction progress. Therapeutic facilities using the Stanford superconducting electron linear accelerator is being built at Stanford, California. All these facilities are expected to be in operation by 1973 or 1974.

Negative π mesons do seem to offer potential advantages in radiation therapy. However, because of the complex nature of this radiation both in terms of its production, as well as its interaction with matter, the amount of work that needs to be done in areas of physical measurements, radiation biology, and clinical work before we can evaluate the potential of this radiation is more complex and expensive when compared to any other radiation that has been tried so far. It must also be stressed that there is a tremendous need for development of better techniques for tumor localization. As Dr. W. E. Powers pointed out, you can hit the object only when you know exactly where it is. The precise location of a tumor (at least in some cases) is not that well known and simultaneous developments of tumor localization is essential in order to take the best advantage of localization characteristics of π^- mesons.

REFERENCES

1. M. A. Bagshaw, H. S. Kaplan, and R. H. Sagerman, Radiology 85, 121 (1965).
2. H. D. Suit, "Introduction: Statement of the Problems Pertaining to the Effect of Dose Fractionation and Total Treatment Time on Response of Tissue to X-Irradiation," in Carmel Conf. Proc. Time and Dose Relationships in Radiation Biology as Applied to Radiotherapy, Brookhaven National Laboratory Report BNL-50203 (C-57), p. vii (1969).
3. M.L.M. Boone, A. L. Wiley, Jr., IEEE Trans. Nucl. Sci. NS-18, 3, 36 (1971).
4. L. H. Gray, Am. J. Roentgenol. 85, 803 (1961).
5. J. F. Fowler, R. L. Morgan, and C.A.P. Wood, Brit. J. Radiol. 34, 77 (1963).
6. L. M. Van Putten and R. F. Kallman, J. Natl. Cancer Inst. 40, 441 (1968).
7. H. S. Kaplan, Radiation Res. 43, 460 (1970).
8. B. G. Karlsson, Strahlentherapie 124, 481 (1964).
9. B. Larsson, Brit. J. Radiol. 34, 143 (1961).
10. P. H. Fowler and D. H. Perkins, Nature 189, 524 (1961).
11. P. H. Fowler and V. M. Mayes, Proc. Phys. Soc. (London) 92, 377 (1967).
12. H. Davis, J. Muirhead and J. N. Woulds, Nucl. Phys. 78, 673 (1966).
13. S. B. Curtis and M. R. Raju, Radiation Res. 34, 239 (1968).
14. M. R. Raju, E. Lampo, S. B. Curtis and C. Richman, "Dosimetry of π^- Mesons Using Scintillation Detectors and Plastic Scintillators," Phys. Med. Biol., 16, 599-610 (1971).
15. A. H. Sullivan and J. Baarli, Phys. Med. Biol. 13, 435 (1968).
16. G. M. Tisljar-Lentulis, G. M. Bond, J. S. Robertons and W. H. Moore, Radiation Res. 46, 17 (1971).
17. J. E. Turner, J. Dutrannois, H. J. Wright, J. Baarli, R. N. Hamm and A. H. Sullivan, "Calculation of Negative and Positive Pion Depth-Dose Curves and Comparison with Experiment, I. Parallel Uniform Beams." CERN Report DI/HP/32 (1970).
18. J. Sperinde, V. Perez-Mendez, A. J. Miller, A. Rindi and M. R. Raju, Phys. Med. Biol. 15, 643 (1970).
19. P. N. Dean and D. M. Holm, "Pion Stopping Region Visualization Experiments." Radiation Res. 48, 201 (1971).
20. T. T. Puck and P. I. Marcus, J. Exp. Med. 53, 653 (1959).
21. M. M. Elkind, Radiology 74, 529 (1960).
22. H. B. Hewitt and C. W. Wilson, Brit. J. Cancer 13, 69 (1959).
23. G. W. Barendsen, Europ. J. Cancer 2, 333 (1966).
24. G. W. Barendsen, Current Topics in Radiation Research, 4, 293. Eds. M. Ebert and A. Howard. (North-Holland, Amsterdam (1968).